Deep Convection in the Subpolar Gyre: Do We Have Enough Data to Estimate Its Intensity?

A.M. Fedorov[3,5,1†,2†], I.L. Bashmachnikov[1,2], D.A. Iakovleva [1,2], D.A. Kuznetsova [1,2], and R.P. Raj[4]

[1] Saint Petersburg State University, 7/9 Universitetskaya nab, St. Petersburg, 199034, Russian Federation

[2] Nansen International Environmental and Remote Sensing Centre, 7, 14$_{th}$ Line V. O., Saint Petersburg

[3] Royal Netherlands Institute for Sea Research (NIOZ), Ocean Systems, Landsdiep 4, 1797TA, Netherlands

[4] NERSC, Nansen Environmental and Remote Sensing Center, Bjerknes Centre for Climate Research, Thormøhlens Gate 47, 5006 Bergen, Norway.

[5]Utrecht University, Institute for Marine and Atmospheric research Utrecht, Princetonplein 5, 3584CC, Utrecht, Netherlands

[†]Organizations in which AMF was employed until 15.02.2022 and made a contribution to the paper.

Corresponding author: Aleksandr Fedorov (aleksandr.fedorov@nioz.nl; a.fedorov@spbu.ru)

Keywords: intensity of deep convection, accuracy, Subpolar North Atlantic, mixed layer depth, number of vertical casts

Key Points:

- The convection intensity in each of the three convective areas of the Subpolar Gyre can be estimated with a minimum of 10 to 50 vertical casts
- A sufficient number of casts was collected only since the mid-2000s
- In the Subpolar Gyre, the convection intensity increased from the mid-2000s to the late 2010s

Abstract

Deep convection in the Subpolar Gyre (SPG) forms a link between the upper and lower limbs of the Atlantic Meridional Overturning Circulation (AMOC). The intensity of convection in ocean studies is usually estimated using mixed layer depth (MLD). Here MLD is derived using vertical profiles of potential density from the gridded ARMOR3D dataset and from in situ observations of the EN4 dataset. Given limited areas of convective chimneys, the robustness of the estimates

from an available set of vertical profiles needs to be verified before accessing mechanisms of interannual variability of deep convection. For reaching this goal, we first outlined three convection domains in the SPG with a high frequency of deep convection events: the southwestern Labrador Sea (L-DC), the central Irminger Sea (I-DC), and the area south of Cape Farewell (F-DC). The minimum number of randomly scattered casts, required to be executed from January to April for a robust estimate of the maximum MLD, depends on the typical area of the convective regions within the domain and forms 50 casts for L-DC, 40 casts for I-DC and 10 casts for F-DC. For the investigated convection domains, a sufficient number of casts were collected for several standalone winters of the late 1990s, while continuous time series of the convection intensity can be obtained only since the mid-2000s.

Plain Language Summary

In this study, we concentrate on the accuracy of our assessments of the interannual variability of the intensity of deep convection in the Subpolar Gyre. Deep convection forms deep water masses further spreading at the intermediate and deep ocean layers south throughout the Atlantic. These waters are replaced by warmer surface waters entering the subpolar regions in the ocean meridional overturning system. The transported heat strongly influences the state of climate at mid- and high latitudes. The intensity of deep convection is typically estimated in oceanography as the winter maximum of the mixed layer depth, which, in the study region, can exceed 2000 m. Winter in situ observations in the Subpolar Gyre are relatively scarce. This raises the question: how robust are the existing estimates of the interannual variability of the convection intensity derived from historical observations, provided the limited size of the areas of deep convection. In this study, we show that for three main convective domains of the Subpolar Gyre (the Labrador Sea, Irminger Sea, and Farewell domain), a minimum of 10 to 50 randomly scattered profiles (depending on the domain) is required for a confident estimate of the deep convection intensity.

Keywords:
intensity of deep convection, accuracy, Subpolar North Atlantic, mixed layer depth, number of vertical casts

1 Introduction

The Atlantic Ocean regulates meridional gradients of upper ocean heat content through a three-dimensional system of its circulation cells, often generalized as a meridional cell of the Atlantic Meridional Overturning Circulation (AMOC), a part of the Global Conveyor (Böning et al., 2006; Born et al., 2016; Broecker, 1991, 1987; Lappo, 1984). Deep convection, which links the upper and lower limbs of the Conveyor in the North Atlantic, is one of the key processes of this circulation pattern (Buckley and Marshall, 2016; Johnson et al., 2019; Kuznetsova and Bashmachnikov, 2021).

In the Northern Hemisphere, regions of deep convection are the Nordic Seas and the North Atlantic Subpolar Gyre (SPG) (Gascard, 1991; Johannessen et al., 1991; Schott and Marshall, 1999). All convective areas are observed with cyclonic gyres by rising isopycnals over the weakly stratified intermediate waters in their central areas (the cold water dome), thus decreasing the thickness of the upper low-buoyancy layer. The interannual intensity of the deep-water formation in the convection sites of the North Atlantic is primarily regulated by oceanic heat and salt advection and by intensive heat release from the sea surface to the atmosphere,

among other factors (Bashmachnikov et al., 2021; Sarafanov et al., 2012). For the Greenland Sea, authors stress the importance of variability of the ice cover and the Atlantic water inflow for the development of convection, while for the Norwegian Sea the ocean-atmosphere heat exchange governs the intensity of convection (Bashmachnikov et al., 2021; Böning et al., 2016; Fedorov et al., 2021; Fedorov and Bashmachnikov, 2020; Glessmer et al., 2014; Moore et al., 2015). In the SPG the mechanisms shaping the interannual variability of deep convection are still under discussion. Here we concentrate on the robustness of our knowledge of the interannual variability of deep convection in the SPG, which forms the basis for further understanding of the mechanisms involved.

Relatively warm and salty waters of the North Atlantic (NAC) and Irminger currents (IC), combined with fresh and cold waters of the East/West Greenland (EGC/WGC) and Labrador currents (LC), form the cyclonic circulation pattern around the Labrador and Irminger seas, which is called the SPG (Fig. 1). The topographically trapped jet-like West/East Greenland, and Labrador currents have a typical current velocity of about 25-40 cm s^{-1}, while the relatively wide and weak Irminger current has a current velocity of about 15 cm s^{-1}.

The intensity of the SPG circulation varies in time, primarily linked to variations of the North Atlantic Oscillations (NAO), a principal pattern of atmospheric variability in the North Atlantic (Bakalian et al., 2007; Langehaug et al., 2012; Lohmann et al., 2009; Pickart et al., 2002; Rhein et al., 2011), as well as to those of the East Atlantic Pattern (EAP), which is the second mode in EOF decomposition of spatio-temporal variability of the atmospheric pressure field in the region (Langehaug et al., 2012). The positive NAO phase leads to the cooling and strengthening of the SPG (Lohmann et al., 2009). As the NAO phase turns negative, a gradual weakening of the SPG circulation is observed, reaching its maximum at a 3.5-year lag (Gladyshev et al., 2018). During recent decades, the overall decrease of the SPG circulation (Belonenko et al., 2018) corresponds to an overall warming of the upper water layer during a gradual decrease of the NAO index observed until the mid-2010s (Iakovleva and Bashmachnikov, 2021, 2019).

Variations in the transport of the warmer (saltier) near-surface subtropical water in the SPG trigger a negative (positive) feedback in the deep convection – upper-ocean advection dynamic system. Growth in the upper-ocean salinity increases water density in the central parts of the Irminger and/or Labrador gyres (partly driven by eddy transport), which results in a more intense deep convection and SPG circulation (Born et al., 2016; Levermann and Born, 2007). An intensified convection drives a further intensification of the SPG circulation. On the longer time scales, a related increase in the deep-water formation rate (Belonenko et al., 2018; Gelderloos et al., 2013) intensifies the AMOC and increases the upper ocean northward transport of subtropical water with a decadal time lag (Kuznetsova and Bashmachnikov, 2021; Lozier et al., 2019). An increase in the upper ocean temperature with advection of the warm subtropical water, on the opposite, decreases water density in the SPG and drives similar negative feedback. Acting in parallel, the integral effect depends on the relative importance of temperature (salinity) anomalies in stabilizing (destabilizing) the water column in the convection regions.

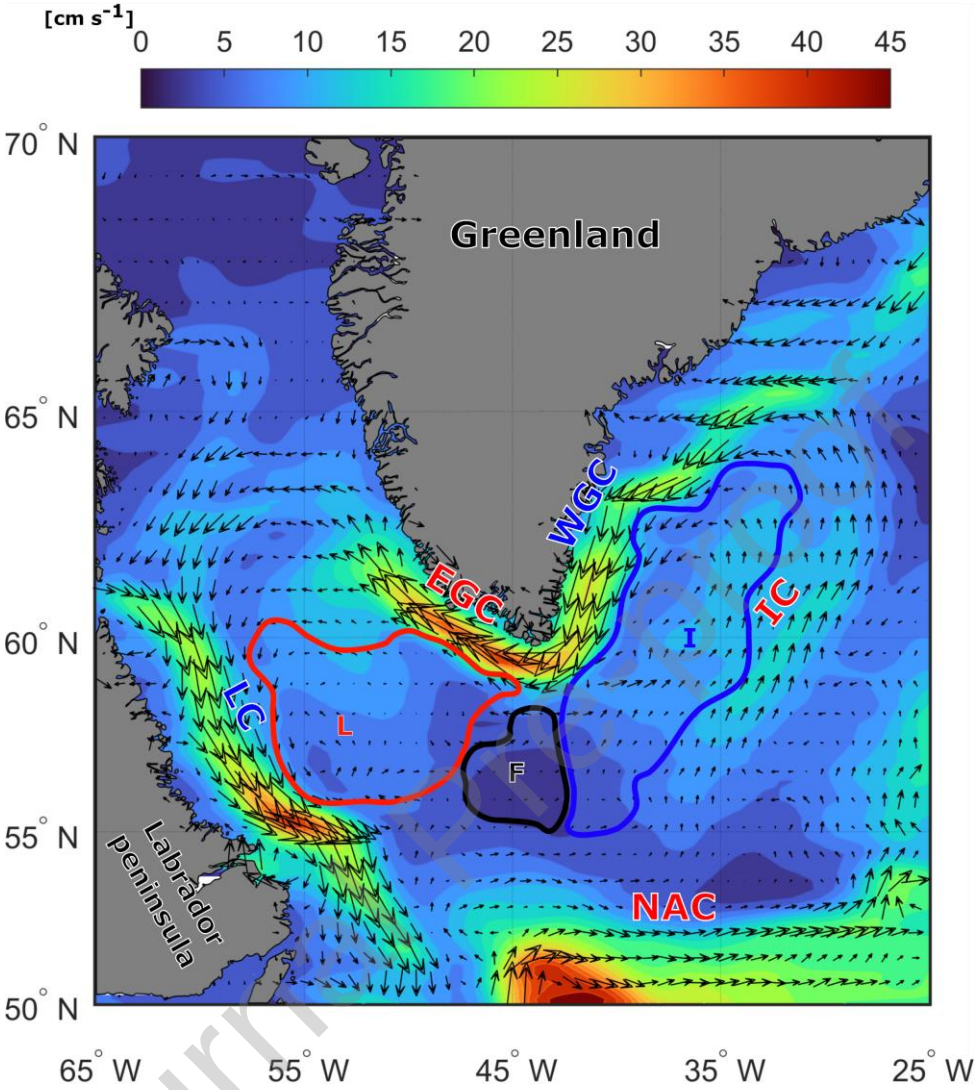

Figure 1. The study region. The mean current velocity (cm s^{-1}) is shown in color; arrows demonstrate the current direction, derived from long-term averaged AVISO altimetry sea-surface height [https://resources.marine.copernicus.eu/product-detail/SEALEVEL_GLO_PHY_L4_MY_008_047/DATA-ACCESS]. Three regions where convection at least once over winters 1993-2019 exceeded 800 m are marked with three solid contours: the convection domain in the Irminger Sea (I) is shown in blue, that of Cape Farewell (F) is shown in black, and that in the Labrador Sea (L) is shown in red. Surface currents: NAC is the North Atlantic Current, IC is the Irminger Current, WGC is the West Greenland Current, EGC is the East Greenland Current and LC is the Labrador Current.

The most frequent development of deep convection in the SPG is observed in three regions (Bashmachnikov et al., 2018; Fedorov et al., 2018): the central Labrador Sea (L-DC), the Irminger Sea (I-DC), and the domain south of Cape Farewell (F-DC) (Fig. 1). These are evident in the animation of the monthly mean mixed layer depth (MLD) (see Supplement S1). This animation suggests that the spatial variability of MLD in each of the selected domains has relatively independent dynamics.

Spatial and temporal variability of deep convection in the Labrador Sea is investigated in a number of publications (Bashmachnikov et al., 2018; Fedorov et al., 2018; Georgiou et al., 2019; Johannessen et al., 1991; Lazier et al., 2002; Schott and Marshall, 1999; Yashayaev, 2007; Yashayaev and Loder, 2017). These in situ and model studies showed that the area of the most frequent convection is situated in the southeastern part of the basin, where, during some winters, the convection depth exceeds 2000 m. However, deep convection over 1000 m was episodically observed to spread almost the whole deep area of the basin. At long time scales, there were obtained some moderate links of the convection intensity with the NAO (Pickart et al., 2002; Rhein et al., 2011) and EAP (Langehaug et al., 2012) atmospheric indices. It was also noted in numerical models that high-frequency atmospheric cooling events can increase the convection intensity during moderate or warm winters (Holdsworth and Myers, 2015). Once formed, the Labrador Sea Water (LSW) is spread over the whole Subpolar Gyre, including the Irminger Sea, at lower mid-depth levels within a year or so (Våge et al., 2011; Yashayaev et al., 2007).

Several decades ago, convection in the Irminger Sea was considered to be of minor importance compared to that in the Labrador Sea. One of the first pieces of evidence of MLD over 1000 m in the Irminger Sea was provided by Bacon et al. (2003), while Pickart et al. (2003) observed a winter MLD of 1500-2000 m. Regular development of deep ocean convection in the I-DC domain was later confirmed in several studies (Bashmachnikov et al., 2019; Fedorov et al., 2018; Fröb et al., 2016; Gladyshev et al., 2016). It was suggested that a certain fraction of the "upper Labrador Sea Water" is formed in the Irminger Sea (Pickart et al., 2003).

Deep convection in the F-DC domain is not that regular and this domain is often (but not always) merged with either L-DC or I-DC (see animation in S1). In the F-DC domain the winter MLDs can reach 1700 m, while an anomalously low stratification of deep waters suggests that this happens relatively regular (Bashmachnikov et al., 2018; Falina et al., 2017; Fedorov et al., 2018; Piron et al., 2017; Rühs et al., 2021; Zunino et al., 2020). However, interannual variability of the convection intensity in this region has never been described. Our analysis below demonstrates that despite a similar decadal variability, in the interannual variability of F-DC we observe notable differences between I-DC and L-DC domains. The reasons for these differences remain to be explored.

In ocean studies, the most common measure of the intensity of convection is the maximum mixed layer depth (MMLD) over the convective season (Kantha and Clayson, 2000). The robustness of this measure is questionable given the limited number of available in situ casts (Fedorov and Bashmachnikov, 2020; Våge et al., 2009). Thus, in 2014/2015, the MMLD in the Irminger Sea from all publicly available in situ data was estimated at 1600 m (Bashmachnikov et al., 2019; de Jong et al., 2018). For the same winter, using a smaller subset of casts from Argo floats, Fröb et al. (2016) estimated the MMLD as 1400 m, while Gladyshev et al. (2016), added their own in situ observations in I-DC (not publically available), estimated the MMLD as 1800 in the central part of the convective domain and 1300 m on its periphery. Similar inconsistencies can be found in various estimates of the convection intensity in the Labrador Sea. The MMLD of 1150 m derived during the winter of 1997 by Lazier et al. (2002) versus 1400 m derived by Pickart et al. (2002) for the same year is a result of using different datasets. During winter 2014, the maximum winter MLD estimated from Argo floats was 1500 m (Holte et al., 2017), 300 m shallower than another estimate of 1800 m from a larger dataset (Yashayaev and Loder, 2017). These inconsistencies mostly do not affect long-term tendencies in the convection intensity

(Holdsworth and Myers, 2015; Våge et al., 2009; Yashayaev and Loder, 2017), but they may become important when analyzing possible mechanisms of year-to-year variations.

The present study primarily aims to answer the following question: how many measurements during the convective season are needed to estimate the year-to-year variability of the deep convection intensity, derived from the maximum MLD, in each of three main deep convection regions of the Subpolar Gyre? Based on these results, we list the range of years when winter measurements available from the open sources provide a sufficiently robust estimate of the intensity of convection in these areas.

2 Data and Methods

The accuracy of the convection intensity derived from estimates of the MMLD naturally depends on the number of available in situ temperature and salinity profiles in the region. These profiles are downloaded from the EN4 dataset (version 2.1, https://www.metoffice.gov.uk/hadobs/en4/download-en4-2-1.html). The dataset contains quality-controlled vertical profiles since 1900, derived from several databases: Argo; World Ocean Database (WOD); Arctic Synoptic Basin Wide Oceanography (ASBO); Global Temperature and Salinity Profile Program (GTSPP). We collected only the profiles with both temperature and salinity which permits the computation of water density profiles used for MLD detection (Bakalian et al., 2007; Born et al., 2016). Raw profiles of temperature and salinity are measured in situ by various instruments including shipboard XCTD, CTD, Argo profiles, and ocean gliders. All casts are quality controlled, duplicates and profiles with unrealistic values of temperature and salinity are filtered out, and the resulting data are interpolated (decimated) to standard ocean levels (Good et al., 2013).

For estimates of typical distributions of the MLD during the convective season, as well as for computation of an alternative measure of convection intensity, the total area with MLD over a predefined threshold (SMLD) (Bashmachnikov et al., 2021; Fedorov and Bashmachnikov, 2020), we use gridded three-dimensional monthly mean ocean temperature and salinity fields from ARMOR3D dataset [https://resources.marine.copernicus.eu/product-detail/MULTIOBS_GLO_PHY_TSUV_3D_MYNRT_015_012]. The data is available since 1993 and has a spatial resolution of ¼° x ¼°. The dataset combines all observed in situ temperature and salinity profiles (from Argo, XCTD, CTD, and moorings) with "synthetic" profiles obtained on a regular grid from remote sensing data (SLA from CMEMS Sea Level, SST from Ostia analyses, SSS from CMEMS MOB). The "synthetic" profiles are obtained by an extrapolation of the sea-surface signals down to 1500 m, using previously derived regional regression equations that link the in situ measured temperature and salinity at different depth levels with the sea surface parameters from the remote sensing data. The final gridded 3D fields combine all available in situ profiles with the "synthetic" profiles in an optimal interpolation procedure (Guinehut et al., 2012). In our previous studies, we cross-validated the interannual variability of the deep convection intensity, measured as the winter MMLD from ARMOR3D, with the MMLD obtained from various ocean reanalyses, as well as convection accesses from various alternative measures (Bashmachnikov et al., 2021, 2019, 2018; Fedorov et al., 2021). The results showed that the long-term tendencies of the MMLD measure using ARMOR3D are consistent between the alternative measures, as well as between the datasets.

The MLD is calculated based on a method suggested by Dukhovskoy (Bashmachnikov et al., 2018; Fedorov et al., 2018). It was found to perform better than the commonly used methods by (Kara, 2003)or (de Boyer Montégut, 2004), especially in the subpolar regions with a weak pycnocline (see, for example, Fig. 3 in Fedorov and Bashmachnikov (2020)). Dukhovskoy's method does not use a predefined threshold, but the MLD is fixed at a depth z where the local vertical potential density gradient $\left|\frac{d\sigma}{dz}\right|$ exceeds by more than two local standard deviations the mean value of the gradient. Following previous studies, we estimated the statistics using the window $[(z-100),\ (z+100)]$. Before implementing this analysis, we filtered the small-scale noise by applying the moving average with a 10 m window and artificially mixed the sections of the profiles with unstable stratification. The final step was a visual control of the algorithm's performance.

3 Results

3.1. Interannual variability of the maximum MLD (MMLD) in the Subpolar Gyre during the convective season

Deep convection in different domains of the SPG occurs during January-May (JFMAM), which is further referred to as the convective season. The peak development of DC is typically in March (Bashmachnikov et al., 2018; Fedorov et al., 2018; Holdsworth and Myers, 2015; Lohmann et al., 2009). For all three convection domains of the SPG (Fig. 1), estimated using the ARMOR 3D dataset, the MMLD shows a similar long-term variability (solid lines in Fig.2), with regular intensive convection reaching 1500-2000 m in the beginning (1993-1996) and at the end (2015-2018) of the study period, and convection of a lower intensity in-between. The weakening of the convection from the 1990s to the 2000s in the Labrador Sea has been previously derived using a relatively independent methodology of analysis of the characteristics and thickness of the LSW at mid-depths (Yashayaev et al., 2007; Yashayaev and Loder, 2017). In particular, it has been shown that a denser Classical LSW, dominating at mid-depths during the 1990s, in the early 2000s was replaced with a lighter Upper LSW. It was also noted, that an episodic bit of deep convection in 2008-2009 did not result in an increase of the Classical LSW at the deep layers, presumably due to a limited period of intensified vertical mixing (Yashayaev and Loder, 2009).

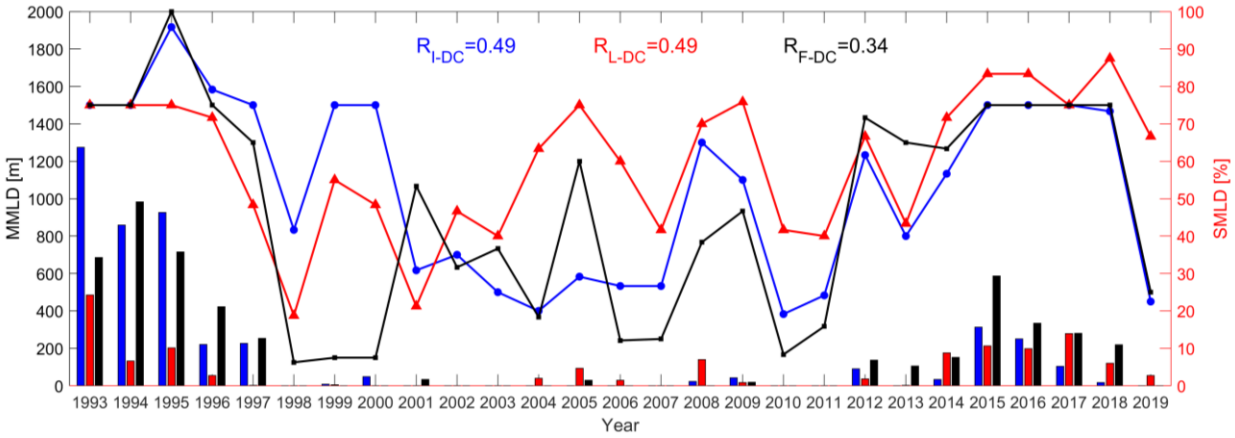

Figure 2. Interannual variability of the MMLD [m] is presented as solid lines (left axis). Interannual variability of the areas with the MLD over 800 m (SMLD), averaged over JFMAM, is presented in [%] of the convection area as vertical bars (right axis). ARMOR 3D data are used. Blue color marks the variables of the I-DC domain; red – for the L-DC domain; black – for the F-DC domain. R_I, R_L, R_F are the correlation coefficients between MMLD and JFMAM mean NAO index in the I-DC, L-DC, and F-DC domains, respectively.

Despite an overall common variability in all three domains of the SPG (for example, the intensified convection during 1993-1996, 2008-2009, 2012, 2014-2018), some years show differences between the domains. During 1999-2000 convection in the F-DC domain was anomalously weak (an MMLD of 200 m), while in L-DC the MMLD reached 800-1200 m, and in I-DC it reached 1400 m. Similarly, during the winters of 2001-2007, the MMLD in the I-DC ranged between 400 and 700 m, notably weaker than that in F-DC during the winters of 2001 and 2005, and significantly weaker than in L-DC during the winters of 2002-2007 (800-1600 m).

Following Fedorov and Bashmachnikov (2020), here we also use a complementary measure of the DC intensity of the total area with MLD over a predefined threshold (SMLD, bars in Fig. 2). This measure can be obtained only from gridded datasets (ARMOR3D data) and compliments the MMLD metrics (see for details Bashmachnikov et al., 2021). In the study region, we define the threshold to be 800 m. This value of this threshold is chosen to be close to the upper limit of the LSW core (Yashayaev and Loder, 2017, 2009). The long-term tendencies in the SMLD (bars in Fig. 2) closely follow those of the MMLD, which supports the robustness of the results.

At the beginning of the study period with deep MMLD (1993-1996), the seasonally averaged SMLD covers 40-65% of the I-DC domain; 35-50% of the F-DC domain; 5-25% of the L-DC domain (Fig. 2). The relatively small percentage of the SMLD in the L-DC domain, compared to that in I-DC and F-DC, is a consequence of a complicated spatial structure of deep convection development in L-DC. Convection during winter was mostly observed in relatively small, isolated regions, the locations of which change from one year to another (Animation S1).

During the following period of 1998-2011, characterized by a relatively shallow MMLD, the SMLD is often close to zero and never exceeds 10% of the outlined convection domains (Fig. 2). During this period, convection, even if occasionally reached big depths, developed as isolated convective chimneys of a relatively small size. The resulting ventilation of the deep water was not intensive and the less dense Upper LSW starts dominating the mid-depths (Yashayaev and Loder, 2017).

For 2015-2018, with the consistent increase of the MMLD in all three domains of the SPG, an increase in the SMLD is also observed. Still, though the MMLD reached the same range of values as in the early 1990s, the SMLD is consistently smaller than at the beginning of the study period: around 5-17% of the I-DC domain, 10-30% of the F-DC domain and 7-12% of the L-DC domains.

Summarizing the results, we see that, in the western SPG (L-DC domain), after weakening during the late 1990s - 2000s, convection practically restore its intensity of the early 1990s. In the eastern SPG (I-DC and F-DC domains), after its weakening in the late 1990s-2000s, convection during the 2010s remains weaker than in the early 1990s. Therefore, there is a

certain long-term tendency for convection in the Irminger Sea and the F-DC domain of the eastern SPG to decrease, which is not the case for the Labrador Sea.

3.2. How many casts do we need?

The intensity of deep convection may be regulated by a number of different mechanisms (Bashmachnikov et al., 2021; Chu and Gascard, 1991; Schott and Marshall, 1999). It is difficult to correctly estimate the contribution of different factors, especially when it is not clear how confident the evaluations of the convection intensity are. Keeping in mind possible biases in estimating the intensity of deep convection from numerical models (Timmermann and Beckmann, 2004), as well as typically limited areas of development of deep convection (Johannessen et al., 1991; Kovalevsky et al., 2020; Yashayaev, 2007), the availability of in situ data remains critical (Fedorov and Bashmachnikov, 2020; van Haren, 2018).

In this section, following Fedorov & Bashmachnikov (2020), we estimate the minimum number of randomly scattered measurements which allows a confident estimate of the MMLD, as a measure of convection intensity, in three SPG domains (Fig. 1). First, using the ARMOR3D dataset, we classify month-to-month variations of the convection development during the JFMAM in the SMLD-MMLD parameter space. For all three domains, the dependencies between SMLD-MMLD parameters are well approximated by the natural logarithmic functions with very similar regression coefficients (Fig. 3 a-c). Using k-means cluster analysis (Arthur and Vassilvitskii, 2007), these results can be split into two clusters. The first one is mostly characterized by variations of the MMLD, while variations of the SMLD in this cluster are small (cluster 1, red dots in Fig 3 a-c). This cluster is typical for situations when deep convection is just developing as one or a few isolated convective chimneys. An example (Fig. 2) is the development of convection in the Labrador Sea during the winters of 2008-2009 (Yashayaev and Loder, 2009). The second cluster is characterized by a gradually varying deep MMLD (1200-2000 m) and a strongly varying SMLD (cluster 2, blue dots in Fig 3 a-c). The k-mean analysis further splits this cluster into two sub-clusters 2a and 2b, with a moderate and large SMLD, respectively. This cluster 2 represents the fully developed convection, which is observed after the merging of isolated chimneys into relatively vast deep convection regions. This was observed during the winters of 1993-1996 and 2015-2018 (see Supplement Fig.S1). To these two types, we should add the third cluster of weak convection (with the MMLD below 800 m), which does not separate in the SMLD-MMLD parameter space since its SMLD is identically zero (by definition). The identified convection types and the SMLD-MMLD dependencies are similar to those obtained earlier for the Greenland Sea (Fedorov and Bashmachnikov, 2020). These dependencies are well described by the logarithmic approximation in the MMLD-SMLD space. Regression equations are the following:

$\mathrm{MMLD} = 11 \times \left(\ln(\mathrm{SMLD}+1)\right)^{1.50}$ for the Irminger convective domain (Fig. 3a),

$\mathrm{MMLD} = 11 \times \left(\ln(\mathrm{SMLD}+1)\right)^{1.80}$ for the Labrador convective domain (Fig. 3b), and

$\mathrm{MMLD} = 11 \times \left(\ln(\mathrm{SMLD}+1)\right)^{1.53}$ for the Farewell convective domain (Fig. 3c).

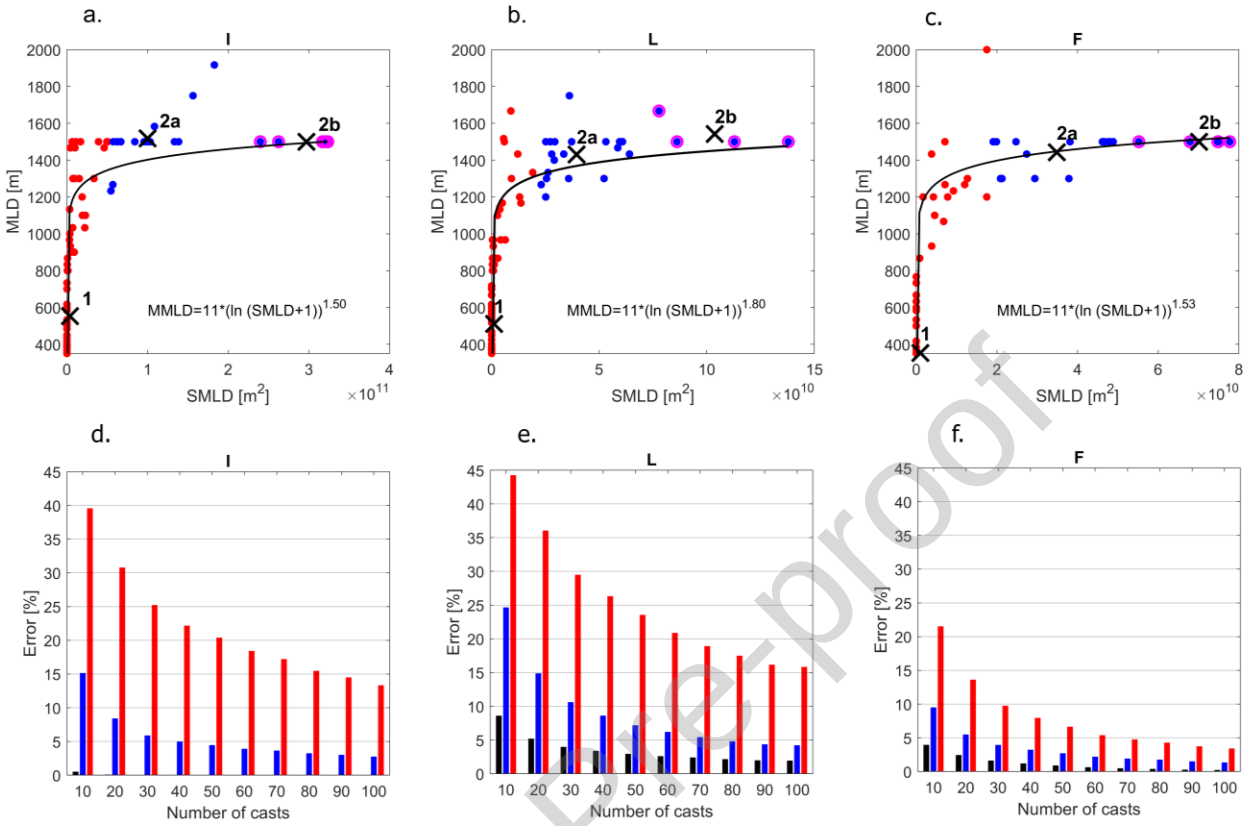

Figure 3. a)-c) The monthly MLD [m] versus the area [m^2] with MLD over 800 m (SMLD) for the JFMAM period. From left to right: the I-DC domain (a); the L-DC domain (b); the F-DC domain (c). Red dots show cluster 1; blue -show cluster 2a, and blue dots with purple rings show cluster 2b. Black lines represent the logarithmic approximation in the MMLD-SMLD space. Black crosses reveal the centers of each cluster. **d)-f)** Errors [%] between the MMLD derived from a random sample of casts (average of 100 experiments) and the real MMLD: black for cluster 1; blue for cluster 2a; red for cluster 2b. From left to right: the I-DC domain (d); the L-DC domain (e); the F-DC domain (f). ARMOR 3D data is used.

For each of the convection domains (Fig. 1) and each cluster (Fig. 3), we constructed artificial MLD distributions (Supplement Fig. S2a-c). Such distributions represent a two-sided hypsographic curve of the derived MLD values, so that the deepest MLD is in the middle and the shallower MLD is shifted towards the periphery. Along X-axis we accumulate the area of the plotted MLD (binned in 100-m bins) averaged over all MLD distributions within a particular cluster. This artificial distribution is an idealized view of the MLD distributions where all the convection domains are merged into a single convective chimney. Over each of these artificial MLD distributions, we randomly scattered a set of a fixed number of casts ranging from 10 to 100 (with an increment of 10). The MMLD error is the difference between the MMLD derived from each of these limited sets and the real MMLD of this particular artificial distribution. Experiments for each fixed number of casts are repeated 100 times to get a representative statistic. The mean (over 100 experiments) MMLD errors are normalized by the real MMLD values and are presented in Figure 3 (d-f) versus the number of casts for clusters 1, 2a, and 2b.

Further, we have chosen the maximum 25% error in the MMLD value as an acceptable threshold accuracy of the MMLD estimate for deriving its interannual variability. Thus, for the MMLD of 1000 m, the error is 250 m.

The analysis showed that 10 casts are sufficient for estimating the MMLD with the 25% error for the developed convection (clusters 2a and 2b, blue and red bars on Fig. 3,e-f). The highest number of casts is naturally needed for narrow chimneys of cluster 1, which is further taken as the threshold for confident MLD estimates. In this case, a 25% error is reached with at least 40 casts scattered over the I-DC domain, 50 casts – over the L-DC domain, and 10 casts – over the F-DC domain. The significantly lower number of casts required in F-DC is explained by the relatively small size of this domain. Provided that during some years the convection may cover large areas (as for convective areas of cluster 2), this minimum number of casts is a certain overestimate. Otherwise, if convection is well developed (cluster 2), 10 randomly scattered casts will be sufficient to reach the 25% accuracy of the MMLD estimate, while when 50 casts are available the MMLD error lowers to 6% of the MMLD value. For example, for 1500 m MMLD this forms around 100 m.

3.3. How many casts do we have?

Based on the criteria derived in the previous section, it is possible to evaluate the potential robustness of the MMLD estimates from the available number of casts during the JFMAM. EN4 dataset provides a relatively complete list of freely available contact measurements, derived from various sources. The total number of EN4 temperature and salinity profiles over the JFMAM period for each of the convection domains (outlined in Fig. 1) are presented in Table 1. The results show that assessing the MMLD in the SPG before 1996 potentially contains large errors, except for 5 years (1968-1972) for the L-DC domain and the year 1963 for the I-DC domain (see Supplement, Table S3). For the altimetry era (after 1993), the MMLD cannot be estimated confidently for 7 years for the I-DC domain, 4 years for the L-DC domain, and 10 years for the F-DC domain (Table 1). The F-DC domain is the least covered with measurements. Noticeable growth in the number of profiles after 2005 is due to the Argo drifter program expansion into the SPG.

Table 1. The number of profiles measured inside deep convection domains annually, based on the EN4 dataset. Red cells show winters (JFMAM) where the criterion of 40 casts is reached in the I-DC domain, 50 casts – in the L-DC domain, and 10 casts – in the F-DC domain. Green cells mark winters when a robust MMLD estimate is possible only if the MLD distribution belongs to cluster 2 (Fig. 3). White cells marked the years when there was an insufficient number of casts for a robust estimate of the MMLD with at least 25% accuracy.

DC domain	93	94	95	96	97	98	99	00	01	02	03	04	05	06	07	08	09	10	11	12	13	14	15	16	17	18	19
I (40)	-	-	-	-	28	84	21	21	37	52	85	24	30	123	74	86	151	550	282	326	1123	776	214	144	228	203	279
L (50)	-	-	-	31	197	230	56	53	16	-	37	332	505	127	98	100	140	188	218	209	295	204	238	217	143	182	160
F (10)	-	-	-	-	-	9	42	-	-	-	16	13	74	-	25	23	24	47	48	74	30	55	32	49	92	36	35

4 Conclusions

The intensity of deep convection is typically estimated using the MMLD derived from in situ data. Model simulations, even the high-resolution ones, are known to mostly overestimate the MMLD (Koenigk et al., 2021; Timmermann and Beckmann, 2004). Our analysis of the accuracy of the convection intensity in three convective domains of the SPG (Fig. 1) shows that 40 casts would be sufficient for providing the MMLD measure with at least 25% accuracy for the Irminger domain (I-DC), 50 casts – for the Labrador domain (L-DC), and 10 casts – for the Farewell domain (F-DC). Considering the available number of casts during the convective season (January to May) in the EN4 dataset, we found that relatively confident estimates of the convection intensity from the MMLD measure in the SPG cannot be obtained earlier than 1996. The amount of data in the SPG increased drastically and become more evenly distributed in time after the mid-2000s, providing robust estimates of the deep convection intensity with the MMLD measure during this modern period. This is a result of the development of the Argo profiling drifter program. The years, when the MMLD measure can be considered robust (Table 1), could be used for further analysis of the mechanisms of the interannual variability of deep convection in the SPG.

The MMLD measure, together with the complementary SMLD measure first introduced by Fedorov and Bashmachnikov (2020), suggest the convection intensity decrease from the 1990s to the 2000s, and a further increase up to the late 2010s, observed in all convective domains of the SPG. These tendencies, derived here using the ARMOR3D dataset, go well with the variability of the convection intensity derived using other methods (Fedorov et al., 2018; Yashayaev and Seidov, 2015).

The joint analysis of MMLD and SMLD variability (Fig. 3), showed that the latter is a more adequate measure of the convection intensity for the fully developed convection, i.e. when individual chimneys expand horizontally and merge into large convective areas (Kovalevsky et al., 2020). At the same time, the winters, when the MMLD was high only locally, i.e. when the SMLD was low, did not result in significant changes in the properties of intermediate and deep waters. Thus, after episodically high MMLD during the winter of 2008-2009, the dominating Upper LSW was not replaced with the Classical LSW, though the latter was observed to dominate the Labrador Sea earlier when such deep mixing was observed over several consecutive winters (Yashayaev and Loder, 2009). This suggests that convection in a limited number of narrow convective chimneys does not have a significant impact on deep-water formation. Therefore, when a gridded dataset is available, the SMLD is a more adequate measure of the intensity of deep convection, keeping in mind that its main dynamic effect is a renewal of intermediate and deep waters.

Acknowledgments

This study was funded by the Ministry of Science and Higher Education of the Russian Federation under project No 13.2251.21.0006 (Unique Identifier RF----225121X0006; Agreement No 075-10-2021-104 in the RF “Electronic Budget” System).

Authorship contribution statement

Fedorov A. M.: Data curation (lead), Formal analysis (lead), Investigation, Visualization, Writing - original draft Preparation, Validation. **Bashmachnikov I.L.**: Conceptualization, Methodology, Supervision, Writing - review & editing (leading), Project Administration, Funding Acquisition. **Iakovleva D.A.**: Data curation (equal), Formal analysis (equal). **Kuznetsova D.A.:** Data curation (equal), Formal analysis (equal). **Raj R.P.:** Conceptualization (supporting), Writing - review & editing (equal).

References

Click or tap here to enter text.

Arthur, D., Vassilvitskii, S., 2007. K-means++: The advantages of careful seeding. Proceedings of the Annual ACM-SIAM Symposium on Discrete Algorithms 07-09-Janu, 1027–1035.

Bacon, S., Gould, W.J., Jia, Y., 2003. Open-ocean convection in the Irminger Sea. Geophys Res Lett 30, 1–4. https://doi.org/10.1029/2002gl016271

Bakalian, F., Hameed, S., Pickart, R., 2007. Influence of the Icelandic Low latitude on the frequency of Greenland tip jet events: Implications for Irminger Sea convection. J Geophys Res 112, C04020. https://doi.org/10.1029/2006JC003807

Bashmachnikov, I.L., Fedorov, A.M., Golubkin, P.A., Vesman, A. v., Selyuzhenok, V. v., Gnatiuk, N. v., Bobylev, L.P., Hodges, K.I., Dukhovskoy, D.S., 2021. Mechanisms of interannual variability of deep convection in the Greenland sea. Deep Sea Research Part I: Oceanographic Research Papers 103557. https://doi.org/10.1016/j.dsr.2021.103557

Bashmachnikov, I.L., Fedorov, A.M., Vesman, A.V., Belonenko, T.V., Dukhovskoy, D.S., 2019. Thermohaline convection in the subpolar seas of the North Atlantic from satellite and in situ observations. Part 2: indices of intensity of deep convection. Sovremennye problemy distantsionnogo zondirovaniya Zemli iz kosmosa 16, 191–201. https://doi.org/10.21046/2070-7401-2019-16-1-191-201

Bashmachnikov, I.L., Fedorov, A.M., Vesman, A.V., Belonenko, T.V., Koldunov, A.V., Dukhovskoy, D.S., 2018. Thermohaline convection in the subpolar seas of the North Atlantic from satellite and in situ observations. Part 1: localization of the deep convection sites. Sovremennye problemy distantsionnogo zondirovaniya Zemli iz kosmosa 15, 184–194. https://doi.org/10.21046/2070-7401-2018-15-7-184-194

Belonenko, T.V., Fedorov, A.M., Bashmachnikov, I.L., Foux, V.R., 2018. Current Intensity Trends in the Labrador and Irminger Seas Based on Satellite Altimetry Data. Izvestiya - Atmospheric and Ocean Physics 54. https://doi.org/10.1134/S0001433818090074

Böning, C.W., Behrens, E., Biastoch, A., Getzlaff, K., Bamber, J.L., 2016. Emerging impact of Greenland meltwater on deepwater formation in the North Atlantic Ocean. Nat Geosci 9, 523–527. https://doi.org/10.1038/ngeo2740

Böning, C.W., Scheinert, M., Dengg, J., Biastoch, A., Funk, A., 2006. Decadal variability of subpolar gyre transport and its reverberation in the North Atlantic overturning. Geophys Res Lett 33, 1–5. https://doi.org/10.1029/2006GL026906

Born, A., Stocker, T.F., Sandø, A.B., 2016. Transport of salt and freshwater in the Atlantic Subpolar Gyre. Ocean Dyn 66, 1051–1064. https://doi.org/10.1007/s10236-016-0970-y

Broecker, W.S., 1991. The Great Ocean Conveyor. Oceanography 4, 79–89.

Broecker, W.S., 1987. Unpleasant surprises in the greenhouse? Nature 328, 123–126. https://doi.org/10.1038/328123a0

Buckley, M.W., Marshall, J., 2016. Observations, inferences, and mechanisms of the Atlantic Meridional Overturning Circulation: A review. Reviews of Geophysics 54, 5–63. https://doi.org/10.1002/2015RG000493

Chu, P.C., Gascard, J.C., 1991. Deep Convection and Deep Water Formation in the Oceans. Elsevier Science.

de Boyer Montégut, C., 2004. Mixed layer depth over the global ocean: An examination of profile data and a profile-based climatology. J Geophys Res 109, C12003. https://doi.org/10.1029/2004JC002378

de Jong, M.F., Oltmanns, M., Karstensen, J., de Steur, L., 2018. Deep convection in the Irminger Sea observed with a dense mooring array. Oceanography 31, 50–59. https://doi.org/10.5670/oceanog.2018.109

Falina, A.S., Sarafanov, A.A., Dobrolubov, S.A., Zapotylko, V.S., Gladyshev, S.V., 2017. Oceanic convection and stratification in the northern atlantic as observed in winter 2013/14. Vestnik Moskovskogo Un. Ser. 5 4, 45–54.

Fedorov, A.M., Bashmachnikov, I.L., 2020. Accuracy of the deep convection intensity from a limited number of casts. Dynamics of Atmospheres and Oceans 92, 101164. https://doi.org/10.1016/j.dynatmoce.2020.101164
Fedorov, A.M., Bashmachnikov, I.L., Belonenko, T.V., 2018. Localization of areas of deep convection in the Nordic seas, the Labrador Sea and the Irminger Sea. Vestnik of Saint Petersburg University. Earth Sciences 63. https://doi.org/10.21638/spbu07.2018.306
Fedorov, A.M., Raj, R.P., Belonenko, T. v., Novoselova, E. v., Bashmachnikov, I.L., Johannessen, J.A., Pettersson, L.H., 2021. Extreme Convective Events in the Lofoten Basin. Pure Appl Geophys. https://doi.org/10.1007/s00024-021-02749-4
Fröb, F., Olsen, A., Våge, K., Moore, G.W.K., Yashayaev, I., Jeansson, E., Rajasakaren, B., 2016. Irminger Sea deep convection injects oxygen and anthropogenic carbon to the ocean interior. Nat Commun 7. https://doi.org/10.1038/ncomms13244
Gascard, J.-C., 1991. Open Ocean Convection and Deep Water Formation Revisited in the Mediterranean, Labrador, Greenland and Weddell Seas. pp. 157–181. https://doi.org/10.1016/S0422-9894(08)70066-7
Gelderloos, R., Katsman, C.A., Våge, K., 2013. Detecting Labrador Sea Water formation from space. J Geophys Res Oceans 118, 2074–2086. https://doi.org/10.1002/jgrc.20176
Georgiou, S., van der Boog, C.G., Brüggemann, N., Ypma, S.L., Pietrzak, J.D., Katsman, C.A., 2019. On the interplay between downwelling, deep convection and mesoscale eddies in the Labrador Sea. Ocean Model (Oxf) 135, 56–70. https://doi.org/10.1016/j.ocemod.2019.02.004
Gladyshev, S. v., Gladyshev, V.S., Gulev, S.K., Sokov, A. v., 2018. Structure and Variability of the Meridional Overturning Circulation in the North Atlantic Subpolar Gyre, 2007–2017. Doklady Earth Sciences 483, 1524–1527. https://doi.org/10.1134/S1028334X18120024
Gladyshev, S. v., Gladyshev, V.S., Gulev, S.K., Sokov, A. v., 2016. Anomalously deep convection in the Irminger Sea during the winter of 2014–2015. Doklady Earth Sciences 469, 766–770. https://doi.org/10.1134/S1028334X16070229
Glessmer, M.S., Eldevik, T., Våge, K., Øie Nilsen, J.E., Behrens, E., 2014. Atlantic origin of observed and modelled freshwater anomalies in the Nordic Seas. Nat Geosci 7, 801–805. https://doi.org/10.1038/ngeo2259
Good, S.A., Martin, M.J., Rayner, N.A., 2013. EN4: Quality controlled ocean temperature and salinity profiles and monthly objective analyses with uncertainty estimates. J Geophys Res Oceans 118, 6704–6716. https://doi.org/10.1002/2013JC009067
Guinehut, S., Dhomps, A.-L., Larnicol, G., le Traon, P.-Y., 2012. High resolution 3-D temperature and salinity fields derived from in situ and satellite observations. Ocean Science 8, 845–857. https://doi.org/10.5194/os-8-845-2012
Holdsworth, A.M., Myers, P.G., 2015. The influence of high-frequency atmospheric forcing on the circulation and deep convection of the Labrador Sea. J Clim 28, 4980–4996. https://doi.org/10.1175/JCLI-D-14-00564.1
Holte, J., Talley, L.D., Gilson, J., Roemmich, D., 2017. An Argo mixed layer climatology and database. Geophys Res Lett 44, 5618–5626. https://doi.org/10.1002/2017GL073426
Iakovleva, D.A., Bashmachnikov, I.L., 2021. On the seesaw in interannual variability of upper ocean heat advection between the North Atlantic Subpolar Gyre and the Nordic Seas. Dynamics of Atmospheres and Oceans 96, 101263. https://doi.org/10.1016/j.dynatmoce.2021.101263
Iakovleva, D.A., Bashmachnikov, I.L., 2019. Interannual variations of heat and freshwater contents in the cold water dome of the Labrador Sea. Vestnik of Saint Petersburg University. Earth Sciences 64, 136–158. https://doi.org/10.21638/spbu07.2019.108
Johannessen, O.M., Sandven, S., Johannessen, J.A., 1991. Eddy-related winter convection in the boreas basin. Elsevier Oceanography Series. https://doi.org/10.1016/S0422-9894(08)70062-X
Johnson, H.L., Cessi, P., Marshall, D.P., Schloesser, F., Spall, M.A., 2019. Recent Contributions of Theory to Our Understanding of the Atlantic Meridional Overturning Circulation. J Geophys Res Oceans 124, 5376–5399. https://doi.org/10.1029/2019JC015330
Kantha, L.H., Clayson, C.A., 2000. Small Scale Processes in Geophysical Fluid Flows, Internatio. ed. Academic Press, San Diego.
Kara, A.B., 2003. Mixed layer depth variability over the global ocean. J Geophys Res 108, 3079. https://doi.org/10.1029/2000JC000736
Koenigk, T., Fuentes-Franco, R., Meccia, V.L., Gutjahr, O., Jackson, L.C., New, A.L., Ortega, P., Roberts, C.D., Roberts, M.J., Arsouze, T., Iovino, D., Moine, M.-P., Sein, D. v., 2021. Deep mixed ocean volume in the Labrador Sea in HighResMIP models. Clim Dyn. https://doi.org/10.1007/s00382-021-05785-x
Kovalevsky, D. v, Bashmachnikov, I.L., Alekseev, G. v, 2020. Formation and decay of a deep convective chimney. Ocean Model (Oxf) 148, 101583. https://doi.org/https://doi.org/10.1016/j.ocemod.2020.101583

Kuznetsova, D.A., Bashmachnikov, I.L., 2021. On the mechanisms of variability of the Atlantic Meridional Overturning Circulation. Oceanology (Wash D C) 61, 1–13.
Langehaug, H.R., Medhaug, I., Eldevik, T., Otterå, O.H., 2012. Arctic/Atlantic exchanges via the subpolar gyre. J Clim 25, 2421–2439. https://doi.org/10.1175/JCLI-D-11-00085.1
Lappo, S.S., 1984. The causes of heat advection to the north across the equator in the Atlantic Ocean. Studies of Processes of Interaction between the Ocean and the Atmosphere 125–129.
Lazier, J., Hendry, R., Clarke, A., Yashayaev, I., Rhines, P., 2002. Convection and restratification in the Labrador Sea, 1990-2000. Deep Sea Res 1 Oceanogr Res Pap 49, 1819–1835. https://doi.org/10.1016/S0967-0637(02)00064-X
Levermann, A., Born, A., 2007. Bistability of the Atlantic subpolar gyre in a coarse-resolution climate model. Geophys Res Lett 34, L24605. https://doi.org/10.1029/2007GL031732
Lohmann, K., Drange, H., Bentsen, M., 2009. Response of the North Atlantic subpolar gyre to persistent North Atlantic oscillation like forcing. Clim Dyn 32, 273–285. https://doi.org/10.1007/s00382-008-0467-6
Lozier, M.S., Li, F., Bacon, S., Bahr, F., Bower, A.S., Cunningham, S.A., de Jong, M.F., de Steur, L., DeYoung, B., Fischer, J., Gary, S.F., Greenan, B.J.W., Holliday, N.P., Houk, A., Houpert, L., Inall, M.E., Johns, W.E., Johnson, H.L., Johnson, C., Karstensen, J., Koman, G., le Bras, I.A., Lin, X., Mackay, N., Marshall, D.P., Mercier, H., Oltmanns, M., Pickart, R.S., Ramsey, A.L., Rayner, D., Straneo, F., Thierry, V., Torres, D.J., Williams, R.G., Wilson, C., Yang, J., Yashayaev, I., Zhao, J., 2019. A sea change in our view of overturning in the subpolar North Atlantic. Science (1979) 363, 516–521. https://doi.org/10.1126/science.aau6592
Moore, G.W.K., Våge, K., Pickart, R.S., Renfrew, I.A., 2015. Decreasing intensity of open-ocean convection in the Greenland and Iceland seas. Nat Clim Chang 5, 877–882. https://doi.org/10.1038/nclimate2688
Pickart, R.S., Straneo, F., Moore, G.W.K., 2003. Is Labrador Sea Water formed in the Irminger basin? Deep Sea Res 1 Oceanogr Res Pap 50, 23–52. https://doi.org/10.1016/S0967-0637(02)00134-6
Pickart, R.S., Torres, D.J., Clarke, R.A., 2002. Hydrography of the Labrador Sea during active convection. J Phys Oceanogr 32, 428–457. https://doi.org/10.1175/1520-0485(2002)032<0428:HOTLSD>2.0.CO;2
Piron, A., Thierry, V., Mercier, H., Caniaux, G., 2017. Gyre-scale deep convection in the subpolar North Atlantic Ocean during winter 2014–2015. Geophys Res Lett 44, 1439–1447. https://doi.org/10.1002/2016GL071895
Rhein, M., Kieke, D., Hüttl-Kabus, S., Roessler, A., Mertens, C., Meissner, R., Klein, B., Böning, C.W., Yashayaev, I., 2011. Deep water formation, the subpolar gyre, and the meridional overturning circulation in the subpolar North Atlantic. Deep Sea Res 2 Top Stud Oceanogr 58, 1819–1832. https://doi.org/10.1016/j.dsr2.2010.10.061
Rühs, S., Oliver, E.C.J., Biastoch, A., Böning, C.W., Dowd, M., Getzlaff, K., Martin, T., Myers, P.G., 2021. Changing Spatial Patterns of Deep Convection in the Subpolar North Atlantic. J Geophys Res Oceans 126. https://doi.org/10.1029/2021JC017245
Sarafanov, A., Falina, A., Mercier, H., Sokov, A., Lherminier, P., Gourcuff, C., Gladyshev, S., Gaillard, F., Daniault, N., 2012. Mean full-depth summer circulation and transports at the northern periphery of the Atlantic Ocean in the 2000s. J Geophys Res Oceans 117. https://doi.org/10.1029/2011JC007572
Schott, F., Marshall, J., 1999. Open-Ocean Convection ' Theory , and Models Observations ,. Reviews of Geophysics 37, 1–64.
Timmermann, R., Beckmann, A., 2004. Parameterization of vertical mixing in the Weddell Sea. Ocean Model (Oxf) 6, 83–100. https://doi.org/10.1016/S1463-5003(02)00061-6
Våge, K., Pickart, R.S., Sarafanov, A., Knutsen, Ø., Mercier, H., Lherminier, P., van Aken, H.M., Meincke, J., Quadfasel, D., Bacon, S., 2011. The Irminger Gyre: Circulation, convection, and interannual variability. Deep Sea Res 1 Oceanogr Res Pap 58, 590–614. https://doi.org/10.1016/j.dsr.2011.03.001
Våge, K., Pickart, R.S., Thierry, V., Reverdin, G., Lee, C.M., Petrie, B., Agnew, T.A., Wong, A., Ribergaard, M.H., 2009. Surprising return of deep convection to the subpolar North Atlantic Ocean in winter 2007-2008. Nat Geosci 2, 67–72. https://doi.org/10.1038/ngeo382
van Haren, H., 2018. Grand Challenges in Physical Oceanography. Front Mar Sci 5, 1–3. https://doi.org/10.3389/fmars.2018.00404
Yashayaev, I., 2007. Hydrographic changes in the Labrador Sea, 1960–2005. Prog Oceanogr 73, 242–276. https://doi.org/10.1016/j.pocean.2007.04.015
Yashayaev, I., Bersch, M., van Aken, H.M., 2007. Spreading of the Labrador Sea Water to the Irminger and Iceland basins. Geophys Res Lett 34, 1–8. https://doi.org/10.1029/2006GL028999
Yashayaev, I., Loder, J.W., 2017. Further intensification of deep convection in the Labrador Sea in 2016. Geophys Res Lett 44, 1429–1438. https://doi.org/10.1002/2016GL071668
Yashayaev, I., Loder, J.W., 2009. Enhanced production of Labrador Sea Water in 2008. Geophys Res Lett 36, L01606. https://doi.org/10.1029/2008GL036162

Yashayaev, I., Seidov, D., 2015. The role of the Atlantic Water in multidecadal ocean variability in the Nordic and Barents Seas. Prog Oceanogr 132, 68–127. https://doi.org/10.1016/j.pocean.2014.11.009
Zunino, P., Mercier, H., Thierry, V., 2020. Why did deep convection persist over four consecutive winters (2015–2018) southeast of Cape Farewell? Ocean Science 16, 99–113. https://doi.org/10.5194/os-16-99-2020

CRediT authorship contribution statement

Fedorov A. M.: Data curation (lead), Formal analysis (lead), Investigation, Visualization, Writing - original draft Preparation, Validation. **Bashmachnikov I.L.**: Conceptualization, Methodology, Supervision, Writing - review & editing (leading), Project Administration, Funding Acquisition. **Iakovleva D.A.**: Data curation (equal), Formal analysis (equal). **Kuznetsova D.A.:** Data curation (equal), Formal analysis (equal). **Raj R.P.:** Conceptualization (supporting), Writing - review & editing (equal).

Declaration of Competing Interest

☒ The authors declare that they have no known competing financial interests or personal relationships that could have appeared to influence the work reported in this paper.